IEEE Access
Multidisciplinary ⋮ Rapid Review ⋮ Open Access Journal

Received July 23, 2019, accepted August 4, 2019, date of publication August 8, 2019, date of current version August 23, 2019.

Digital Object Identifier 10.1109/ACCESS.2019.2933913

Electromagnetic Bandgap Backed Millimeter-Wave MIMO Antenna for Wearable Applications

AMJAD IQBAL[1], (Student Member, IEEE), ABDUL BASIR[2], (Student Member, IEEE), AMOR SMIDA[3,4], NAZIH KHADDAJ MALLAT[5], (Senior Member, IEEE), ISSA ELFERGANI[6], JONATHAN RODRIGUEZ[6], (Senior Member, IEEE), AND SUNGHWAN KIM[7]

[1]Centre for Wireless Technology, Faculty of Engineering, Multimedia University, Cyberjaya 63100, Malaysia
[2]Department of Biomedical Engineering, Hanyang University, Seoul 15588, South Korea
[3]Department of Medical Equipment Technology, College of Applied Medical Sciences, Majmaah University, Al Majmaah 11952, Saudi Arabia
[4]Faculty of Mathematical, Physical and Natural Sciences of Tunis, Unit of Research in High Frequency Electronic Circuits and Systems, Tunis El Manar University, Tunis 2092, Tunisia
[5]College of Engineering, Al Ain University of Science and Technology, Al Ain 64141, United Arab Emirates
[6]Instituto de Telecomunicações, Campus Universitário de Santiago, 3810-193 Aveiro, Portugal
[7]Department of Electrical and Electronic Engineering, University of Ulsan, Ulsan 44610, South Korea

Corresponding author: Sunghwan Kim (sungkim@ulsan.ac.kr)

This work was supported in part by the Research Program through the National Research Foundation of Korea under Grant NRF-2016R1D1A1B03934653 and Grant NRF-2019R1A2C1005920, and in part by the Deanship of Scientific Research at Majmaah University under Project RGP-2019-32.

ABSTRACT A millimeter-wave (mm-Wave) multiple input multiple output (MIMO) antenna operating at 24 GHz (ISM band), suitable for wearable applications, is proposed in this paper. The proposed MIMO antenna consists of two elements, designed with an edge-to-edge distance of 5.14 mm, backed by a 5×5 cell electromagnetic bandgap (EBG) structure. The antenna is fabricated on a flexible Rogers 6002 material ($\epsilon_r = 2.94, tan\delta = 0.0012, thickness = 0.254\ mm$). The proposed antenna retains its performance when bent along the x-axis and y-axis. The performance of the antenna in term of s-parameters and radiation properties is studied in free space as well as on a human phantom. Good impedance matching of the antenna at the resonating frequency (24 GHz) is observed when it is bent and when worn on the body. The introduction of the EBG improves the gain by 1.9 dBi, reduces the backward radiation by 8 dB, reduces the power density on the back towards the body from $>$ 200 W/m^2 to $<$ 10 W/m^2, and also enhances the 10 dB bandwidth by 100 MHz. The antenna possesses a low envelope correlation coefficient (ECC) of 0.24, high diversity gain (DG) of 9.7 dB, reasonable multiplexing efficiency of −0.684 dB and a good peak gain of 6 dBi at 24 GHz. The proposed antenna is suitable for wearable applications at mm-Wave range due to its simple geometry and good performance in bending and on-body worn scenarios.

INDEX TERMS Wearable antenna, on-body antenna, mm-Wave antenna, MIMO, s-parameters.

I. INTRODUCTION

Nowadays, wearable networks are seen as the research topic that is most often focused upon; it offers great potential for improving the delivery and monitoring of healthcare systems, sporting performance, navigation, and military usage [1]. Antennas are the key components in the design and successful deployment of wearable networks. Worth noting in this respect is that microstrip patch antennas (MPA) are of special interest: they are more suitable for wearing than other types of antennas due to their peculiar characteristics of lightness, flexibility and conformability when worn [2]. Two major properties: the conformability and level of the specific absorption rate (SAR) of a wearable antenna may be thoroughly checked before employing it in the service of any network. However, at higher frequencies (greater than 6 GHz) the electromagnetic (EM) waves do not penetrate deep into the body and spread over the skin. Therefore, instead of SAR, the ICNIRP, FCC, and IEEE have standardized the exposure limits on the basis of spatial power density (PD = 10 W/m^2).

The associate editor coordinating the review of this article and approving it for publication was Yang Yang.

Designing and operating MPAs for on-body worn applications is a challenging task due to their backward radiation, which harms human tissue [3]. Excess of EM radiations traveling through tissues is converted into heat because of the lossy nature of the tissues. This issue can dramatically diminish the efficiency of the wireless device as well as causes a critical hazard to the wearer's safety. Effective isolation between the antenna and the human body is therefore highly recommended. An electromagnetic bandgap (EBG) structure is a standout amongst the best-known successful approaches to keep wearers safe from the inconvenient impact of such radiation by reduces the level of back-radiation from the antenna and hence reducing the radiation absorbed by the body [4]. The EBG is used to generate in-phase reflection and to suppress the surface waves, which ameliorates the gain of the antenna and reduces human exposure in terms of SAR [5].

Wearable antennas are designed on a flexible substrate because there is a possibility of being crumpled or bent when the person wearing them moves or changes his/her state. Maintaining the good performance of the antennas throughout their use is challenging and should be investigated. To achieve flexibility and conformeability for wearable devices, researchers have used conductive fabrics, liquid materials, flexible elastomerous substrates like PDMS, and mesh like structures of the cladding [6]–[8]. Because the human body is not flat, so some part of the wearable devices including antennas have to bend to aligned with the body shape. Additionally, the daily life activities of the wearer causes the components of the wearable devices to undergo crumpling and stretching. However, techniques like using fabrics, elastorous substrates, and meshed structures increase the complexity of integration and soldering, and decrease the durability of the components. The effects of bending on the performance of both conventional and high impedance structure integrated patch antennas are briefly discussed in [9]. Additionally, symmetrical bending along the x-axis and y-axis is performed in [10] in order to investigate the effects of bending on the antenna's performance. Also, an irregular crumpled wearable antenna is studied in [11].

The performance of wearable antennas is dramatically degraded when operated on a uniform (flat smooth) or non-uniform (curved and rough) human body. In fact, severe multipath fading, due to reflections/scatterings around and on the human body is experienced in on-body communication links, which can dramatically reduce the robustness and reliability of communication [12]. To enhance the clarity of communication under the influence of multipath fading, it is highly recommended to use a diversity technique such as multiple-input-multiple-output (MIMO) [13], [14]. A dual polarized, two element MIMO antenna operating at WLAN band is proposed in [15]. A wideband two element MIMO antenna with reduced SAR value and good diversity performance in a smart watch for wireless applications is investigated in [16]. A dual-port single element MIMO antenna for an ISM band is reported in [17] for wearable applications. All the aforementioned studies of MIMO wearable studies are carried out at lower frequencies, moreover, they did not provide the bending and crumpling effects analysis. Additionally, they clearly missed the reduction of coupling between the elements and human safety analysis, which is very important in wearable cases.

Due to the increasing demand for 5G wearable IoTs, designing millimeter-wave (mm-Wave) antennas have attracted the interest of many researchers, but none of them consider wearable scenarios for diversity application (MIMO). Moreover, the higher frequency EM radiations are more hazardous for health, there is an intend need to shield the body from the excess exposure of these EM-waves. The presented paper, however, proposes a two port, two element MIMO antenna operating at mm-Wave (24 GHz) range for wearable applications. The antenna is backed by EBG, which reduce the back radiations from the antenna and reduce the power densities (PD) on the body, additionally, increases the gain of the antenna. The antenna has good performance in on-body worn scenarios in term of conformability and spatial power density. The main contribution of this paper may be summarized as follows:

- To the best of our knowledge, this is the first ever paper to focus on the design of the mm-Wave MIMO antenna for wearable applications.
- Detailed analysis of the proposed antenna under deforming conditions and also on the human body show acceptable performance.
- The proposed antenna has good gain, efficiency, and low spatial power density.

II. ANTENNA DESIGN AND ANALYSIS

A. ANTENNA DESIGN

A rectangular shaped patch with flexible substrate and full ground plane for 24 GHz has been suggested. A 50Ω transmission line along with λ/4 matching stub is used for feeding the patch antenna. Rogers 6002 ($\epsilon_r = 2.94$, $tan\delta = 0.0012$, $thickness = 0.254\ mm$) is used as a substrate for the proposed design. Initially, a rectangular patch antenna operating at 24 GHz was designed. In the second step, the same antenna is used for designing a two element multiple-input multiple-output (MIMO) antenna system (Fig. 1a). The two elements are placed with an edge-to-edge distance of 5.14 mm.

B. ELECTROMAGNETIC BANDGAP (EBG) DESIGN

Antenna parameters such as gain, radiation efficiency and operating bandwidth are greatly affected by surface waves and near field coupling. One of the convenient ways to suppress the surface waves and near field coupling is to introduce a high impedance structure, such as the electromagnetic bandgap (EBG) [4]. The EBG in the present study was designed at 24 GHz to tackle the problem induced by near field coupling and surface waves. A unit cell of the proposed EBG is shown in Fig. 1c. The unit cell was analyzed for its constitutive parameters [permittivity (ϵ) and permeability (μ)] using the technique discussed in [18]. The following

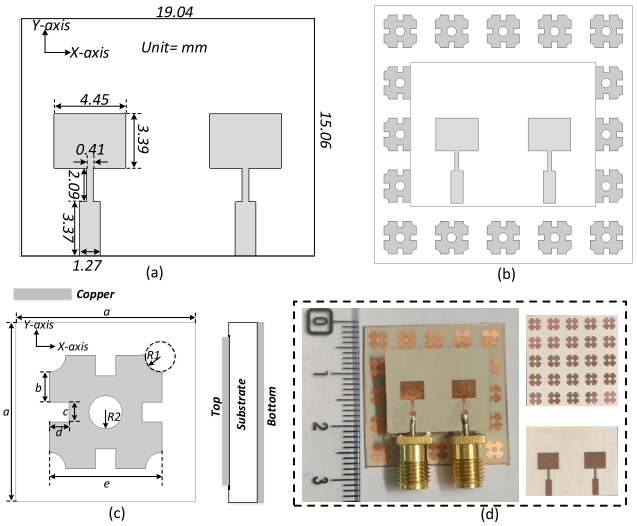

FIGURE 1. (a) Top view of the multiple-input multiple-output (MIMO) antenna, (b) top view of the MIMO antenna with 5×5 EBG, (c) top and side veiw of EBG ($a = 5.4$ mm, $b = 0.9$ mm, $c = d = 0.6$ mm, $R1 = R2 = 0.5$ mm, and $e = 3.4$ mm), and (d) fabricated prototype.

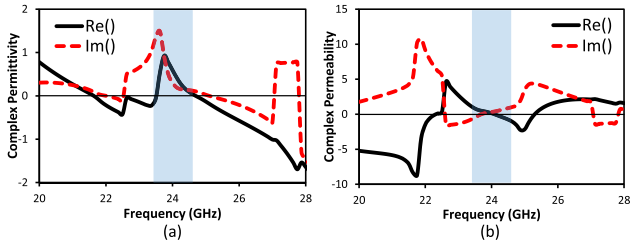

FIGURE 2. Extracted parameters of the EBG cell (a) complex permittivity, and (b) complex permeability.

equations [Eqs. (1)-(4)] were used to extract the permittivity and permeability.

$$z = \pm\sqrt{\frac{(1+S_{11})^2 - S_{21}^2}{(1-S_{11})^2 - S_{21}^2}} \tag{1}$$

$$e^{j\eta k_\circ d} = \frac{S_{21}}{1 - S_{11}\dfrac{z-1}{z+1}} \tag{2}$$

$$\epsilon = \frac{\eta}{z} \tag{3}$$

$$\mu = \eta \times z \tag{4}$$

where z is the normalized impedance, S_{11} is the reflection coefficient, S_{21} is the transmission coefficient, η is the refractive index, $k_\circ$ is the wave number, d is the thickness of the substrate, ϵ is the effective permittivity and μ is the effective permeability. The extracted permittivity and permeability of the EBG cell is illustrated in Fig. 2. We can see that permittivity of EBG cell is near to zero in the band of interest, while permeability is zero at 24 GHz. The permittivity or permeability of material tends to zero means zero refractive index [as obvious from Eqs. (3)-(4)] [19].

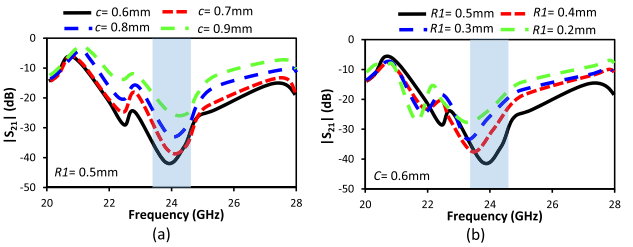

FIGURE 3. Simulated transmission coefficient (S_{21}) of the 5×5 EBG array for varying (a) *c*, and (b) *R1*.

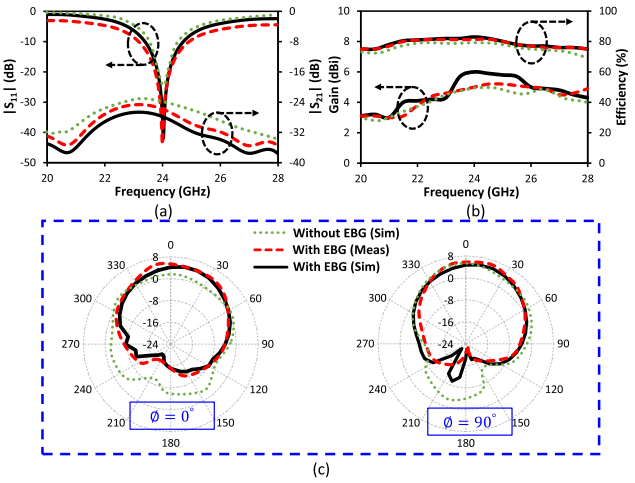

FIGURE 4. Simulated (with and without EBG) and measured (with EBG) (a) s-parameters, (b) gain and efficiency, and (c) radiation pattern at 24 GHz.

A 5×5 cells array was evaluated before implementing it in an antenna design. A 5×5 EBG array was designed and a 50Ω transmission line was placed above it for the initial evaluation of the EBG array. The reason for placing a 50Ω transmission line was to observe the stopband performance of the EBG array. To obtain optimal results, a number of simulations were performed by varying the EBG parameters such as *c* and *R1*. Fig. 3 shows the effect of EBG's varying parameters on the stopband performance of the EBG array. Parameters *c* and *R1* impacted on the magnitude of the S_{21} of EBG array and also shifted the stopband range. The optimized EBG structure and its parameters are given in Fig. 1c. The EBG stopband performance at 24 GHz was achieved by finely tuning the EBG parameters.

C. EBG BACKED MIMO ANTENNA

For analyzing EBG backed antenna, a 5×5 unit cells were placed below the 2 element MIMO antenna, as shown in Fig. 1b. The simulated and measured reflection coefficient, radiation pattern, gain and efficiency are given in Fig. 4. The EBG structure act as a near-zero-index (NZI) metamaterial structure and hence blocks the transmission of the magnetic field in the near field region [20]. It increases the far-field radiation directivity due to near-zero refractive index and

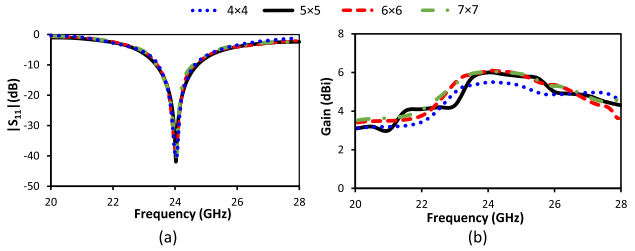

FIGURE 5. Impact of number of EBG cells on (a) reflection coefficient of the antenna, and (b) gain of the antenna.

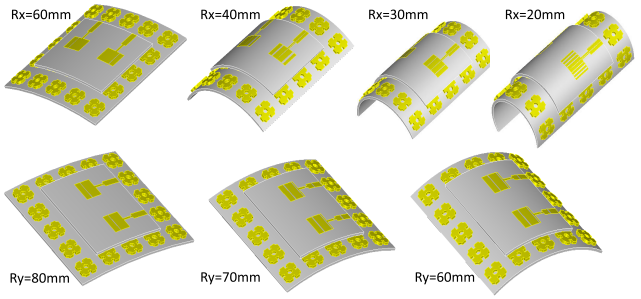

FIGURE 6. Structurally deformed proposed antenna with different values of the curvature radius, ranging from Rx = 20 mm to 60 mm along the x-axis and from Ry = 60 mm to 80 mm along the y-axis.

also enhance the gain due to in phase reflection. The gain is further enhanced due to the cavity effect generated by the gap between the antenna and EBG layer. The coupling of the antennas is mainly due to surface waves or near-field reactive coupling [21], [22]. The isolation can be enhanced by reducing the surface waves or near-field reactive coupling. EBG in this design reduce the near-field magnetic coupling and hence reduce the mutual coupling of the antenna. The efficiency of the antenna is enhanced due to the reduction of near-field coupling. It can be observed from Fig. 4a that the reflection coefficient at 24 GHz is −25 dB for conventional antenna while it is −42 dB for the EBG backed antenna. The 10-dB simulated bandwidth of the conventional antenna is noted as 700 MHz, whereas the EBG backed antenna had an 800 MHz bandwidth. EBG has also an impact on the transmission coefficient (S_{21}) of the antenna. The S_{21} of the antenna went down from −31 dB to −37 dB. The introduction of the EBG also affected the gain, efficiency and backward radiation of the antenna. The antenna gain was enhanced from 4.1 dBi to 6 dBi, as shown in Fig. 4b. Also, the efficiency of the antenna improved from 76.7% to 80.5%. The backward radiation in both principal planes was reduced (11 dB in $\phi = 0°$ and 18 dB in $\phi = 90°$) by employing EBG with the antenna. The spatial power density was reduced by significant level through the EBG array. The effect of number of unit cells on the performance of the antenna is shown in Fig. 5. The reflection coefficient and gain of the antenna were studied for 4×4, 5×5, 6×6, and 7×7 EBG cells. The reflection coefficient of the antenna was same for all cases. The gain of the antenna was dependent on the number of

TABLE 1. Comparison of the conventional and EBG backed antenna.

Parameters	Conventional Antenna	EBG backed Antenna
Resonant Frequency (GHz)	24	24
Bandwidth (MHz)	700	800
Mutual Coupling (dB)	-31	-37
Gain (dBi)	4.1	6
Directivity (dBi)	3.35	7.45
Efficiency (%)	76.7	80.5
Backward Radiation (dB)	-6 at $\phi = 0°$ plane -4 at $\phi = 90°$ plane	-17 at $\phi = 0°$ plane -22 at $\phi = 90°$ plane

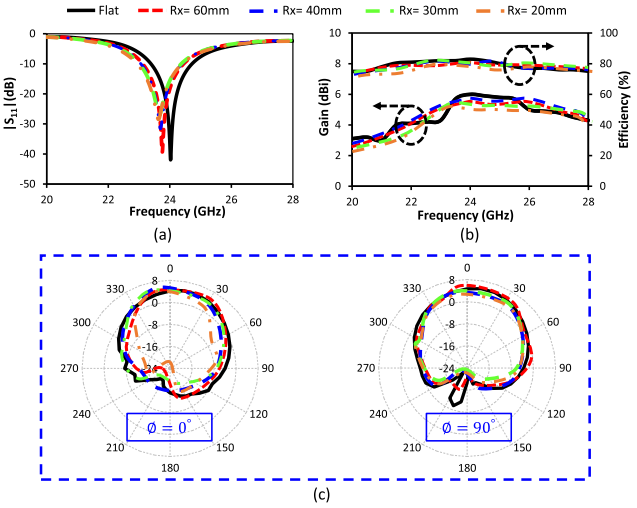

FIGURE 7. Simulated (bended along x-axis) (a) reflection coefficient, (b) gain and efficiency, and (c) radiation pattern at 24 GHz.

EBG cells. The gain of the antenna had direct relation with the number of EBG cells. However, the gain improvement was negligible by increasing the EBG cells beyond 5×5. The EBG cells which were located away from the antenna had very less impact on the performance of the antenna [23] and hence there is no significant change even if the EBG cells were 7×7. A detailed discussion of spatial power density is given in Section III-C. The performance of the antenna with and without the EBG array is summarized in Table. 1.

III. ANTENNA ANALYSIS FOR WEARABLE APPLICATIONS

A. BENDING ANALYSIS

In body area networks (BAN), a wearable antenna is expected to bend and crumple while it is in use. The performance of the proposed antenna when bent in Rx (along the x-axis) and Ry (along the y-axis) was investigated in order to ensure its suitability for being worn. Fig. 6 shows the bending radii for Rx and Ry bending. The antenna was investigated for four different radii (20, 30, 40 and 60 (Unit = mm)) along the x-axis (Rx) and three radii (60, 70 and 80 (Unit = mm)) along the y-axis (Ry). A range of radii for bending (along the x-axis and y-axis) was chosen because human arms and legs vary in size. Fig. 7 and 8 shows the impact of different bending radii on the reflection coefficient of the antenna. The antenna performed well under different bending conditions in both planes (x-axis and y-axis) as is evident from Fig. 7 and 8.

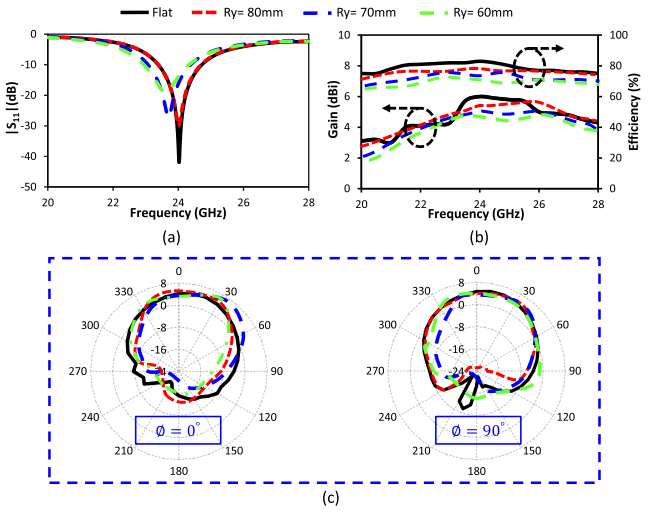

FIGURE 8. Simulated (bended along y-axis) (a) reflection coefficient, (b) gain and efficiency, and (c) radiation pattern at 24 GHz.

TABLE 2. Comparison of antenna properties, bent along x-axis and along y-axis.

Bending along x-axis					
Rx (mm)	Flat	60	40	30	20
Gain (dBi)	6	5.9	5.6	6	5.8
Efficiency	80.2 %	79.01 %	77.4 %	77.6 %	74.2 %
Bending along y-axis					
Ry (mm)	Flat	80	70	60	
Gain (dBi)	6	5.5	5.47	5.36	
Efficiency	80.2 %	75.6 %	72.6 %	69.8 %	

The bending radii had very little impact on the resonant frequency of the antenna. The resonant frequency shifted to 23.71 GHz from 24 GHz without changing the bandwidth, for an extreme case when the antenna was bent to 20 mm along the x-axis (Fig. 7a). A small impedance mismatch and shift in frequency was observed when the antenna was deformed along the y-axis. The resonant frequency shifted to 23.65 GHz with a deformation radius of 60 mm along the y-axis, as shown in Fig. 8a. The measured reflection coefficient of the antenna in both bending condition (along x-axis and y-axis) is illustrated in Fig. 10a-b. The gain and efficiency of the antenna when bent are reported in Fig. 7b and 8b. The radiation pattern of the antenna for both deformation scenarios (along the x-axis and along y-axis) is reported in Fig. 7c and 8c. A summary of the antenna performance when bent along the x-axis and y-axis is given in Table. 2.

B. HUMAN BODY LOADING

The antenna performance on the human body is reported in this section. The antenna was tested on different parts of the human body (chest, leg and arm) using a realistic human model and the results were investigated. The EBG structure was used in this antenna because this structure allows less backward radiation. A excellent and stable reflection coefficient besides the radiation characteristics was observed, as illustrated in Fig. 9. The measured reflection coefficient

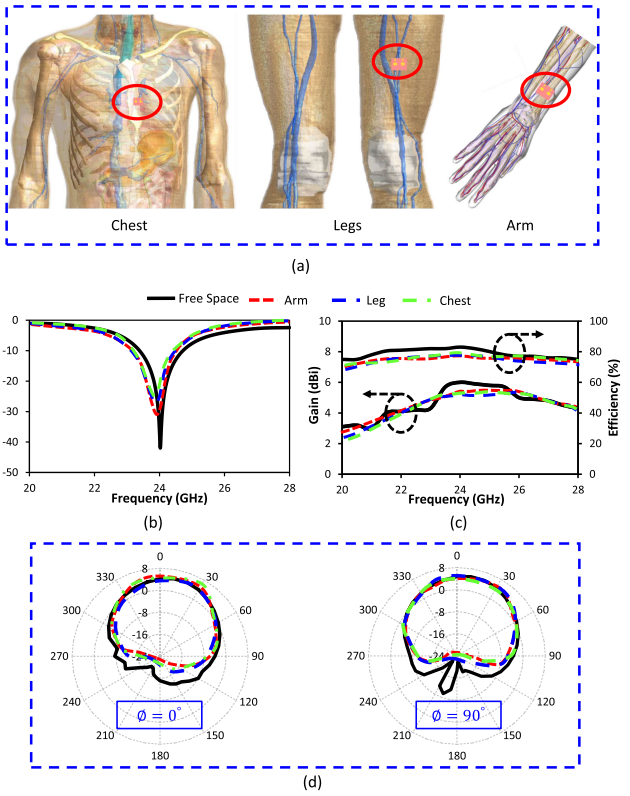

FIGURE 9. (a) Antenna placed on chest, leg and arm, (b) simulated reflection coefficient, (c) simulated gains and efficiencies, and (d) simulated radiation patterns at 24 GHz.

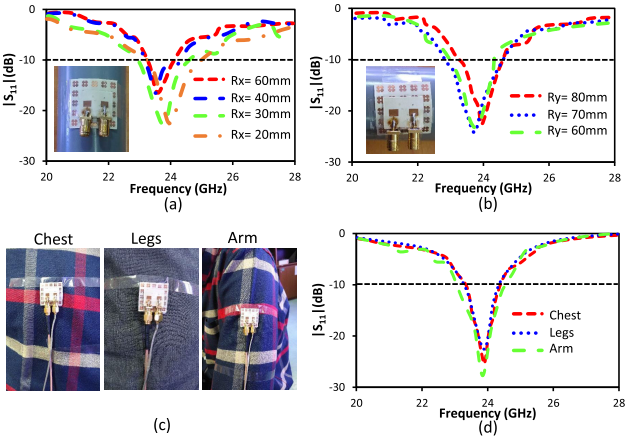

FIGURE 10. (a) Measured reflection coefficient of the antenna along x-axis, (b) measured reflection coefficient of the antenna along y-axis, (c) antenna performance evaluation at chest, legs and arm, and (d) measured reflection coefficient of the antenna on chest, legs and arm.

of the antenna in case of human body loading is shown in Fig. 10d.

C. SPATIAL POWER DENSITY (PD) ANALYSIS

A microstrip patch antenna radiates most of its power in the bore direction and only small portion of radiated power is leaked from the back. This leaked radiated power is absorbed by the body when the antenna is operated in the vicinity of the

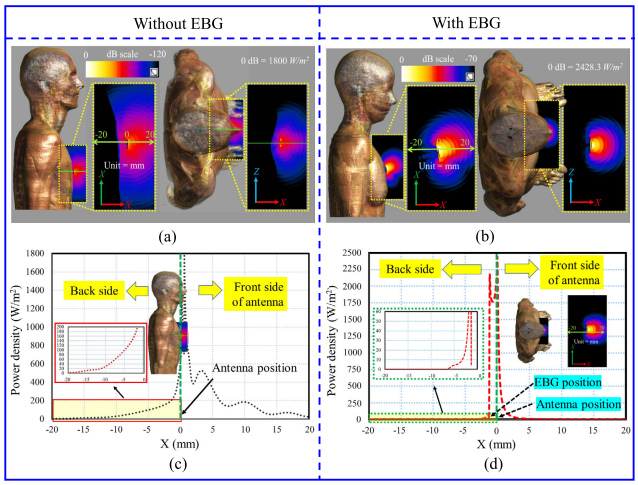

FIGURE 11. Spatial power density (a) without EBG, (b) with EBG, (c) without EBG for varied distance *X*, and (d) with EBG for varied distance *X*.

human body. EM waves are hazardous to human health if certain limits of exposure are exceeded. To ensure public safety, these limits are set by electromagnetic field (EMF) regulating authorities: the International Commission on Non-ionizing Radiation Protection (ICNIRP), IEEE, and the Federal Communication Commission (FCC). Currently, the EMF exposure level for lower frequencies below 3 GHz, 6 GHz and 10 GHz is assessed by the specific absorption rate (SAR, W/kg) under IEEE, FCC, and ICNIRP regulations, respectively [24], [25]. However, at higher frequencies the wavelength becomes shorter and the penetration of the EM waves into the human body is negligibly shallow. Most of the EM waves concentrate and spread over the skin; hence, the SAR is no longer effectively applicable for the evaluation of public safety [26], [27]. As shown in Table. 3, the ICNIRP, FCC, and IEEE have standardized the exposure limits on the basis of spatial power density (PD = 10 W/m^2) at above 10 GHz, 6 GHz and 3 GHz, respectively. To ensure public safety, we analyzed our antenna when it was worn on the body. First, we mounted the antenna on the chest of a real duke model and then analysed it with EBG, as shown in Fig. 9a. The spatial power densities (PD) were numerically calculated for both conditions (without and with EBG) at an input power of 1 W, as depicted in Fig. 11. The peak PDs were 1800 W/m^2 without EBG and 2428.3 W/m^2 with EBG. Fig. 11a and 11b show the spatial distribution of PD without and with EBG. From Figs. 11c and 11d, it is evident that to operate the proposed antenna within safety limits at an input power of 1 W, the antenna should be placed 15 mm and 1.9 mm away from the human body for without and with EBG case, respectively. However, in practical the radiated power of the transmitter also has certain restriction, because the Maximum Effective Isotropic Radiated Power (EIRP) is in the mW range, which is far smaller than 1W. If the proposed antenna is backed with EBG and input power is in the mW range, it is safe even when placed just over the skin.

TABLE 3. Public safety restrictions for electromagnetic exposure.

	Transition Freq. (GHz)	Power density limit (W/m^2)	Localized SAR limit below transition Freq. (W/kg)
FCC	6	10	1.6 (Averaged over 1g)
IEEE	10	10	2 (Averaged over 10g)
ICNIRP	3	10	

IV. MIMO PERFORMANCE

In this section, the MIMO performance of the proposed antenna is studied. The proposed MIMO antenna has two elements placed at a distance of 5.14 mm from each other. The performance of the MIMO antenna is investigated in terms of reflection coefficient, isolation, Envelope Correlation Coefficient (ECC), Diversity Gain (DG), Multiplexing efficiency (η_{Mux}) and peak gain (PG).

A. REFLECTION COEFFICIENT AND ISOLATION

The simulated and measured reflection and transmission coefficients of the proposed mm-Wave antenna with and without EBG structure are plotted in Fig. 4. It is quite obvious from the figure that the simulated and measured results accord well. The proposed antenna operates at 24 GHz with 10-dB BW of 800 MHz. It can be seen that the impedance matching is enhanced by adding an EBG structure to the antenna. In designing a MIMO antenna system, it is always desirable to check the mutual coupling between the MIMO elements. Fig. 4a shows the simulated and measured S_{21} results for the proposed MIMO antenna. It is clear from the figure that the mutual coupling between the MIMO elements is significantly lower: the S_{21} is below -37 dB at 24 GHz. Such lower transmission coefficients confirm that the MIMO elements are significantly isolated from the adjacent elements, which confirms the suitability of the proposed wearable mm-Wave MIMO system for use in WBAN applications.

B. ENVELOPE CORRELATION COEFFICIENT (ECC)

Computation of the envelope correlation coefficient (ECC) for any MIMO system is important for determining how different the individual elements of the MIMO system are from each other in terms of the antenna's individual properties. The ECC value should be equal to zero for an uncorrelated MIMO antenna system; however, MIMO antenna systems with an ECC value of less than 0.5 are considered acceptable. The far-field radiation pattern [Equation. (5)] is used for calculating the ECC for the given MIMO antenna system [28].

$$ECC = \frac{|\int\int_{4\pi}(\vec{M}_i(\theta,\phi)) \times (\vec{M}_j(\theta,\phi))\, d\Omega|^2}{\int\int_{4\pi}|(\vec{M}_i(\theta,\phi))|^2\, d\Omega \int\int_{4\pi}|(\vec{M}_j(\theta,\phi))|^2\, d\Omega} \quad (5)$$

where $\vec{M}_i(\theta,\phi)$ describe the 3D radiation pattern when antenna i is excited and $\vec{M}_j(\theta,\phi)$ describe the 3D radiation pattern when antenna j is excited. The solid angle in Equation (5) is represented as Ω. ECC value varies from 0.19 to 0.24 over the operational band, while an ECC value of 0.24 is observed at the resonant frequency (24 GHz) when the antenna is laid flat. The ECC of the antenna when bent (along the x-axis and y-axis) is evaluated and reported

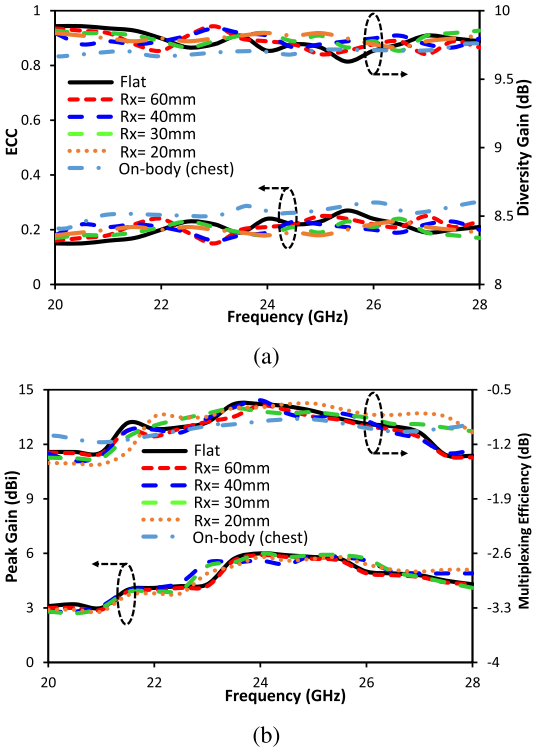

FIGURE 12. MIMO parameters in Rx bending and human body loading conditions (a) ECC and diversity gain, and (b) peak gain and multiplexing efficiency.

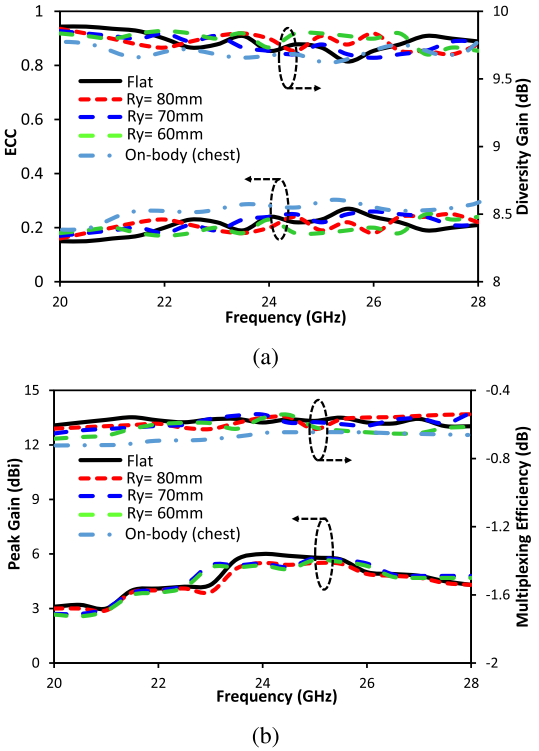

FIGURE 13. MIMO parameters in Ry bending and human body loading conditions (a) ECC and diversity gain, and (b) peak gain and multiplexing efficiency.

in Fig. 12a and 12b. ECC values of 0.21, 0.19, 0.18, and 0.18 were observed for the antenna bent along the x-axis at radii of 60, 40, 30 and 20 mm, respectively, at 24 GHz (Fig. 12a). ECC values of 0.2, 0.24, and 0.23 were observed for the antenna bent along the y-axis at radii of 80, 70 and 60 mm, respectively (Fig. 13a). It can be concluded from these two figures that the antenna's ECC remains in an acceptable range even when bent. The ECC of the antenna was 0.25–0.3, when the antenna was placed on the body.

C. DIVERSITY GAIN (DG)

Another important parameter for any MIMO antenna system is diversity gain. It shows how much the transmitted power is reduced using any diversity scheme. Diversity gain (DG) for any MIMO antenna system can be calculated by means of the following relation [28].

$$DG = 10\sqrt{1 - (ECC)^2} \tag{6}$$

Fig. 12a shows the antenna diversity gain for an antenna bent along the x-axis. A 9.7 dB diversity gain was noted at 24 GHz for the unbent antenna. Diversity gains of 9.77, 9.81, 9.83 and 9.83 dB were noted for the antenna bent at 60, 40, 30 and 20 mm, respectively at 24 GHz along the x-axis (Fig. 12a). Diversity gains of 9.79, 9.70, and 9.73 dB were noted for the antenna bent at 80, 70, and 60 mm, respectively at 24 GHz along the y-axis (Fig. 13a). The diversity gain of the antenna in the on-body worn scenario is almost 9.7 dB.

D. MULTIPLEXING EFFICIENCY

The multiplexing efficiency for the proposed MIMO antenna was calculated using the following relation [29], [30].

$$\eta_{Mux} = \sqrt{(1 - |\rho|^2)\eta_1\eta_2} \tag{7}$$

where η_1, η_2 and ρ represent the efficiency of element 1, the efficiency of element 2 and the complex envelope correlation coefficient between the two elements ($\rho \approx |ECC|^2$), respectively. An unbent antenna has a multiplexing efficiency (η_{Mux}) of -0.684 dB at 24 GHz. η_{Mux} for an antenna bent along the x-axis and y-axis is given in Fig. 12b and 13b, respectively. The value of η_{Mux} at 24 GHz remains in reasonable range for all the scenarios in which the antenna is bent. The η_{Mux} of the antenna in the on-body worn scenario is near to -0.85 dB.

E. PEAK GAIN

The peak gain of the proposed MIMO antenna for different bending radii against frequency is given in Fig. 12b and 13b. A peak gain of 6 dBi was observed for the flat antenna. A peak gain of 5.9, 5.6, 6 and 5.8 dBi was observed at 24 GHz for the bending radii (along the x-axis) of 60, 40, 30 and 20 mm respectively. A peak gain of 5.5, 5.47, and 5.36 dBi was observed at 24 GHz for the bending radii (along the y-axis) of 80, 70 and 60 mm respectively.

V. CONCLUSION

This paper presents a high performance MIMO antenna at mm-Wave range (24 GHz) for wearable applications. The proposed MIMO antenna consists of two elements, designed at edge-to-edge distance of 5.14 mm backed by a 5×5 cells electromagnetic bandgap (EBG) structure. Good impedance matching at the resonating frequency (24 GHz) is observed for the antenna in bending and on-body worn scenario. The introduction of the EBG improves the gain by 1.9 dBi, reduces the backward radiation by 8 dB, reduces the power density and enhances the 10-dB bandwidth by 100 MHz. The antenna possesses a low envelope correlation coefficient (ECC) of 0.24, high diversity gain (DG) of 9.7 dB, reasonable multiplexing efficiency of −0.684 dB and a good peak gain of 6 dBi at 24 GHz. The proposed antenna is suitable for wearing applications at the mm-Wave range, thanks to its simple geometry and good capacity to operate when bent and worn on the body.

REFERENCES

[1] N. F. M. Aun, P. J. Soh, A. A. Al-Hadi, M. F. Jamlos, G. A. E. Vandenbosch, and D. Schreurs, "Revolutionizing wearables for 5G: 5G technologies: Recent developments and future perspectives for wearable devices and antennas," *IEEE Microw. Mag.*, vol. 18, no. 3, pp. 108–124, May 2017.

[2] P. S. Hall and Y. Hao, "Antennas and propagation for body centric communications," in *Proc. 1st Eur. Conf. Antennas Propag. (EuCAP)*, Nov. 2006, pp. 1–7.

[3] M. Wang, Z. Yang, J. Wu, J. Bao, J. Liu, L. Cai, T. Dang, H. Zheng, and E. Li, "Investigation of SAR reduction using flexible antenna with metamaterial structure in wireless body area network," *IEEE Trans. Antennas Propag.*, vol. 66, no. 6, pp. 3076–3086, Jun. 2018.

[4] R. Das and H. Yoo, "Application of a compact electromagnetic bandgap array in a phone case for suppression of mobile phone radiation exposure," *IEEE Trans. Microw. Theory Techn.*, vol. 66, no. 5, pp. 2363–2372, May 2018.

[5] G.-P. Gao, B. Hu, S.-F. Wang, and C. Yang, "Wearable circular ring slot antenna with EBG structure for wireless body area network," *IEEE Antennas Wireless Propag. Lett.*, vol. 17, no. 3, pp. 434–437, Mar. 2018.

[6] R. B. V. B. Simorangkir, Y. Yang, L. Matekovits, and K. P. Esselle, "Dual-band dual-mode textile antenna on PDMS substrate for body-centric communications," *IEEE Antennas Wireless Propag. Lett.*, vol. 16, pp. 677–680, 2017.

[7] R. B. V. B. Simorangkir, Y. Yang, K. P. Esselle, and B. A. Zeb, "A method to realize robust flexible electronically tunable antennas using polymer-embedded conductive fabric," *IEEE Trans. Antennas Propag.*, vol. 66, no. 1, pp. 50–58, Jan. 2018.

[8] R. C. Webb, A. P. Bonifas, A. Behnaz, Y. Zhang, K. J. Yu, H. Cheng, M. Shi, Z. Bian, Z. Liu, Y.-S. Kim, W.-H. Yeo, J. S. Park, J. Song, Y. Li, Y. Huang, A. M. Gorbach, and J. A. Rogers, "Ultrathin conformal devices for precise and continuous thermal characterization of human skin," *Nature Mater.*, vol. 12, no. 10, pp. 938–944, 2013.

[9] P. Salonen and Y. Rahimat-Samii, "Textile antennas: Effects of antenna bending on input matching and impedance bandwidth," *IEEE Aerosp. Electron. Syst. Mag.*, vol. 22, no. 3, pp. 10–14, Mar. 2007.

[10] M. A. B. Abbasi, S. S. Nikolaou, M. A. Antoniades, and M. N. Stevanović, and P. Vryonides, "Compact EBG-backed planar monopole for BAN wearable applications," *IEEE Trans. Antennas Propag.*, vol. 65, no. 2, pp. 453–463, Feb. 2017.

[11] B. Hu, G.-P. Gao, L.-L. He, X.-D. Cong, and J.-N. Zhao, "Bending and on-arm effects on a wearable antenna for 2.45 GHz body area network," *IEEE Antennas Wireless Propag. Lett.*, vol. 15, pp. 378–381, 2016.

[12] D. Wen, Y. Hao, M. O. Munoz, H. Wang, and H. Zhou, "A compact and low-profile MIMO antenna using a miniature circular high-impedance surface for wearable applications," *IEEE Trans. Antennas Propag.*, vol. 66, no. 1, pp. 96–104, Jan. 2018.

[13] T. Hassan, M. U. Khan, H. Attia, and M. S. Sharawi, "An FSS based correlation reduction technique for MIMO antennas," *IEEE Trans. Antennas Propag.*, vol. 66, no. 9, pp. 4900–4905, Sep. 2018.

[14] S. S. Jehangir and M. S. Sharawi, "A wideband sectoral Quasi-Yagi MIMO antenna system with multibeam elements," *IEEE Trans. Antennas Propag.*, vol. 67, no. 3, pp. 1898–1903, Mar. 2019.

[15] L. Qu, H. Piao, Y. Qu, H.-H. Kim, and H. Kim, "Circularly polarised MIMO ground radiation antennas for wearable devices," *Electron. Lett.*, vol. 54, no. 4, pp. 189–190, Feb. 2018.

[16] C.-H. Wu, J.-S. Sun, and B.-S. Lu, "Watchstrap-embedded four-element multiple-input–multiple-output antenna design for a smartwatch in 5.2–5.8 GHz wireless applications," *Int. J. Antennas Propag.*, vol. 2018, Feb. 2018, Art. no. 1905984.

[17] H. Li, S. Sun, B. Wang, and F. Wu, "Design of compact single-layer textile MIMO antenna for wearable applications," *IEEE Trans. Antennas Propag.*, vol. 66, no. 6, pp. 3136–3141, Jun. 2018.

[18] D. R. Smith, S. Schultz, P. Markoš, and C. M. Soukoulis, "Determination of effective permittivity and permeability of metamaterials from reflection and transmission coefficients," *Phys. Rev. B, Condens. Matter*, vol. 65, no. 19, Apr. 2002, Art. no. 195104.

[19] P. K. Panda and D. Ghosh, "Isolation and gain enhancement of patch antennas using EMNZ superstrate," *AEU-Int. J. Electron. Commun.*, vol. 86, pp. 164–170, Mar. 2018.

[20] R. Mark, N. Rajak, K. Mandal, and S. Das, "Metamaterial based superstrate towards the isolation and gain enhancement of MIMO antenna for WLAN application," *AEU-Int. J. Electron. Commun.*, vol. 100, pp. 144–152, Feb. 2019.

[21] Z. Qamar, U. Naeem, S. A. Khan, M. Chongcheawchamnan, and M. F. Shafique, "Mutual coupling reduction for high-performance densely packed patch antenna arrays on finite substrate," *IEEE Trans. Antennas Propag.*, vol. 64, no. 5, pp. 1653–1660, May 2016.

[22] A. Iqbal, O. A. Saraereh, A. Bouazizi, and A. Basir, "Metamaterial-based highly isolated MIMO antenna for portable wireless applications," *Electronics*, vol. 7, no. 10, p. 267, 2018.

[23] F. Yang and Y. Rahmat-Samii, *Electromagnetic Band Gap Structures in Antenna Engineering*. Cambridge, U.K.: Cambridge Univ. Press, 2009.

[24] A. Basir, A. Bouazizi, M. Zada, A. Iqbal, S. Ullah, and U. Naeem, "A dual-band implantable antenna with wide-band characteristics at MICS and ISM bands," *Microw. Opt. Technol. Lett.*, vol. 60, no. 12, pp. 2944–2949, 2018.

[25] A. Bouazizi, G. Zaibi, A. Iqbal, A. Basir, M. Samet, and A. Kachouri, "A dual-band case-printed planar inverted-F antenna design with independent resonance control for wearable short range telemetric systems," *Int. J. RF Microw. Comput.-Aided Eng.*, vol. 29, no. 8, p. e21781, 2019.

[26] D. Colombi, B. Thors, and C. Törnevik, "Implications of EMF exposure limits on output power levels for 5G devices above 6 GHz," *IEEE Antennas Wireless Propag. Lett.*, vol. 14, pp. 1247–1249, 2015.

[27] K. Zhao, Z. Ying, and S. He, "EMF exposure study concerning mmWave phased array in mobile devices for 5G communication," *IEEE Antennas Wireless Propag. Lett.*, vol. 15, pp. 1132–1135, 2016.

[28] M. S. Sharawi, *Printed Mimo Antenna Engineering*. Norwood, MA, USA: Artech House, 2014.

[29] R. Tian, B. K. Lau, and Z. Ying, "Multiplexing efficiency of MIMO antennas," *IEEE Antennas Wireless Propag. Lett.*, vol. 10, pp. 183–186, 2011.

[30] A. Iqbal, O. A. Saraereh, A. W. Ahmad, and S. Bashir, "Mutual coupling reduction using F-shaped stubs in UWB-MIMO antenna," *IEEE Access.*, vol. 6, pp. 2755–2759, 2018.

AMJAD IQBAL (S'18) received the degree in electrical engineering from the COMSATS Institute of Information Technology, Islamabad, Pakistan, in 2012, and the M.S degree in electrical engineering from the Department of Electrical Engineering, CECOS University of IT and Emerging Science, Peshawar, Pakistan, in 2018. He is currently pursuing the Ph.D. degree with the Faculty of Engineering, Multimedia University, Cyberjaya, Malaysia. He worked as a Lab Engineer with the Department of Electrical Engineering, CECOS University, Peshawar, from 2016 to 2018. His research interests include printed antennas, flexible antennas, implantable antennas, MIMO antennas, dielectric resonator antennas, and synthesis of microwave components.

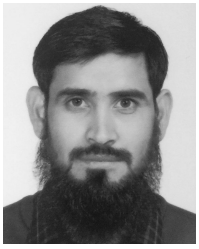

ABDUL BASIR (S'17) was born in Khyber Pukhtoonkhwa, Pakistan, in 1989. He received the B.Sc. degree in telecommunication engineering from the University of Engineering and Technology, Peshawar, Pakistan, in 2015. He is currently pursuing the M.S. leading to the Ph.D. degree in biomedical engineering with the Hanyang University, Seoul, South Korea. His research interests include implantable antennas and systems, biomedical circuits, wearable antennas, MIMO communication, metamaterial, dielectric resonator antennas, reconfigurable antennas, long range wireless power transfer, and wireless charging of biomedical implants.. He was awarded Silver Prize for the Best Student Paper in Student Paper Contest 2018, Seoul section. He was also awarded with Third Prize for the Best Student Paper Completion 2018 by the Korea Communications Agency (KCA) and Korean Institute of Electromagnetic Engineering and Science (KIEES).

AMOR SMIDA received the degree in electronic baccalaureate, in 2008, the M.Sc. degree in analyze and digital processing of the electronic systems, in 2010, and the Ph.D. degree from the Faculty of Mathematical, Physical and Natural Sciences of Tunis, Tunis El-Manar University, Tunisia, in 2014. From 2008 to 2014, he was a Graduate Student Researcher with the Unit of Research in High Frequency Electronic Circuits and Systems. Since August 2014, he has been an Assistant Professor with the Department of Medical Equipment Technology, College of Applied Medical Sciences, Majmaah University, Saudi Arabia. His current research interests include smart antennas, biosensors, biomedical applications, neural network applications in antennas, adaptive arrays, and microwave circuits design CST studio microwave.

NAZIH KHADDAJ MALLAT (M'07–SM'12) received the Bachelor of Engineering degree in electrical and electronics engineering from "Lebanese University—Lebanon", in 2000, the master's degree from "Ecole Nationale Supérieure des Télécommunications de Bretagne (ENSTB)–France," in 2002, and the Ph.D. degree in telecommunications from the "University of Quebec, Institut National de la Recherche Scientifique (INRS)–Canada," in 2010.

After his Ph.D. and until January 2012, he was Postdoctoral Fellow with the Ecole Polytechnique de Montreal. In 2013, he joined the College of Engineering at "Al Ain University of Science and Technology (AAU)," "United Arab Emirates (UAE)," where he was the Head of "Networks and Communication Engineering and Computer Engineering" Department, from 2013 to 2017; the Deputy Dean of the College of Engineering, from 2014 to 2015; the Dean of the College of Engineering, from September 2015 to March 2018. He has been the Director of the "Quality Assurance and Institutional Research Center," since April 2018. His main research interests include passive microwave/millimeter-wave circuit design and telecommunication systems. He authored or coauthored over 40 publications, mostly focused in multi-port applications, millimeter-wave circuits, antennas, and telecommunications systems.

Dr. Khaddaj Mallat is also a member of the Ordre des Ingénieurs du Québec. He has acquired extensive teaching experience at both undergraduate and graduate levels. He has effectively taught many courses, and their relevant practical elements in laboratories at multiple Montreal universities (ETS, TELUQ, and Ecole Polytechnique de Montreal). The "Fonds Québécois de la Recherche sur la Nature et les Technologies-FQRNT," a granting agency of the Quebec government, has awarded him two prestigious scholarships for his doctoral studies, in 2008, as a Postdoctoral Researcher, from 2010 to 2011, and thanks to his highest level of achievement. He is also the Founder of the IEEE AAU Student Branch and the IEEE UAE MTT-S Chapter (and later the IEEE UAE MTT-S &; IM-S &; AP-S Joint Chapter). He was the Vice-Chair of the IEEE Montreal Section, from 2007 to 2008; a Membership Development Chair, from 2009 to 2010; a Section Chair from 2011 to 2012. He has served also in the steering committee for many IEEE international conferences. He was the IEEE UAE Technical Activities Coordinator, from 2015 until 2018, and the IEEE Region eight Chapter Coordination Subcommittee (ChCSC) Chair, in 2015 and 2016. He was the Organizing Committee Chair of three major events held at Al Ain University of Science and Technology: The 1st IEEE International Workshop at AAU, in February 2014, the 11th IEEE UAE Student Day (hosted for the 1st time by AAU), in May 2016, and the 16th Mediterranean Microwave Symposium (MMS2016), in November 2016.

ISSA ELFERGANI received the M.Sc. and Ph.D. degree in electrical and electronic engineering from the University of Bradford, U.K., in 2008 and 2012, respectively, with a specialization in tunable antenna design for mobile handset and UWB applications. He is currently a Senior Researcher with the Instituto de Telecomunicações, Aveiro, Portugal, working with several national and international research funded projects, such as ENIAC ARTEMIS from 2011 to 2014; EUREKA BENEFIC from 2014 to 2017; CORTIF from 2014 to 2017; GREEN-T from 2011 to 2014; VALUE from 2016 to 2016; H2020-SECRET Innovative Training Network from 2017 to 2020. Since his Ph.D. graduation, he has successfully completed the supervision of several Master and Ph.D. students. He has around 100 high-impact publications in academic journals and international conferences; in addition, he is the author of two book editorial and nine book chapters. He has been on the technical program committee of a large number of IEEE conferences. He has several years of experience in 3G/4G and 5G radio frequency systems research with particular expertise on several and different antenna structures along with novel approaches in accomplishing a size reduction, low cost, improved bandwidth, and gain and efficiency. His expertise include research in various antenna designs, such as MIMO, UWB, balanced and unbalanced mobile phone antennas, RF tunable filter technologies, and power amplifier designs. In 2014, he received prestigious FCT fellowship for his Postdoctoral Research. He is also the IEEE and an American Association for Science and Technology (AASCIT) member. He reviewed several good ranked journals, such as the IEEE Antennas and Wireless Propagation Letters, the IEEE Transactions on Vehicular Technology, IET Microwaves, Antennas and Propagation, IEEE Access, Transactions on Emerging Telecommunications Technologies, *Radio Engineering Journal*, IET-SMT, the *IET Journal of Engineering*. He was the Chair of both 4th and 5th International Workshop on Energy Efficient and Reconfigurable Transceivers (EERT). He is also a Guest Editor of Hindawi special issue *"Antenna Design Techniques for 5G Mobile Communications and Electronics"* special issue on *"Recent Technical Developments in Energy-Efficient 5G Mobile Cells."*

JONATHAN RODRIGUEZ received the master's degree (Hons.) in electronic and electrical engineering and the Ph.D. degree from the University of Surrey, U.K., in 1998 and 2004, respectively. In 2005, he became a Researcher at the Instituto de Telecomunicações, Portugal, where he was a member of the Wireless Communications Scientific Area. In 2008, he became a Senior Researcher, where he established the 4TELL Research Group targeting next-generation mobile systems. Since 2009, he has been serving as an Invited Assistant Professor with the University of Aveiro, Portugal, and an attained Associate Level, in 2015. In 2017, he was appointed as a Professor of mobile communications with the University of South Wales, U.K. He is currently the coordinator of the H2020-MSCA-SECRET Innovative Training Network. He is the author of more than 500 scientific works, including 11 book editorials. He has served as Project Coordinator for major international research projects, including Eureka LOOP and FP7 C2POWER while serving as a Technical Manager for FP7 COGEU and FP7 SALUS. His professional affiliations include Chartered Engineer (CEng), since 2013, and a fellow of the IET, in 2015.

SUNGHWAN KIM received the B.S., M.S., and Ph.D. degrees from Seoul National University, South Korea, in 1999, 2001, and 2005, respectively. He was a Postdoctoral Visitor with the Georgia Institute of Technology (GeorgiaTech), from 2005 till 2007, and a Senior Engineer with Samsung Electronics, from 2007 till 2011. He is currently an Associate Professor with the School of Electrical Engineering, University of Ulsan, South Korea. His main research interests include channel coding, modulation, massive MIMO, visible light communication, and quantum information.